Supplementary Information for

Optical Imaging of Chemically and Geometrically Controlled Interfacial Diffusion and Redox in 2D van der Waals Space

Haneul Kang and Sunmin Ryu*

Department of Chemistry, Pohang University of Science and Technology (POSTECH), Pohang, Gyeongbuk 37673, Korea.

*Correspondence to: sunryu@postech.ac.kr

This PDF file includes:

Supplementary Figures (S1 to S9)
Supplementary Table (S1)

Supplementary Figures

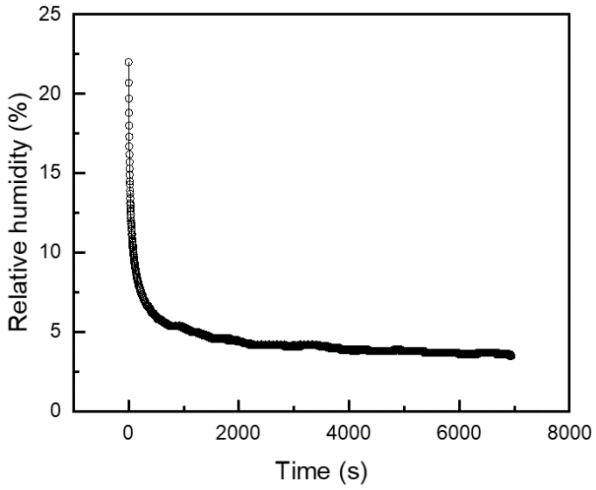

Figure S1. Change of relative humidity in the optical cell. Dry Ar gas was introduced at 1,000 mL min^{-1} to the air-equilibrated optical gas cell at the time zero.

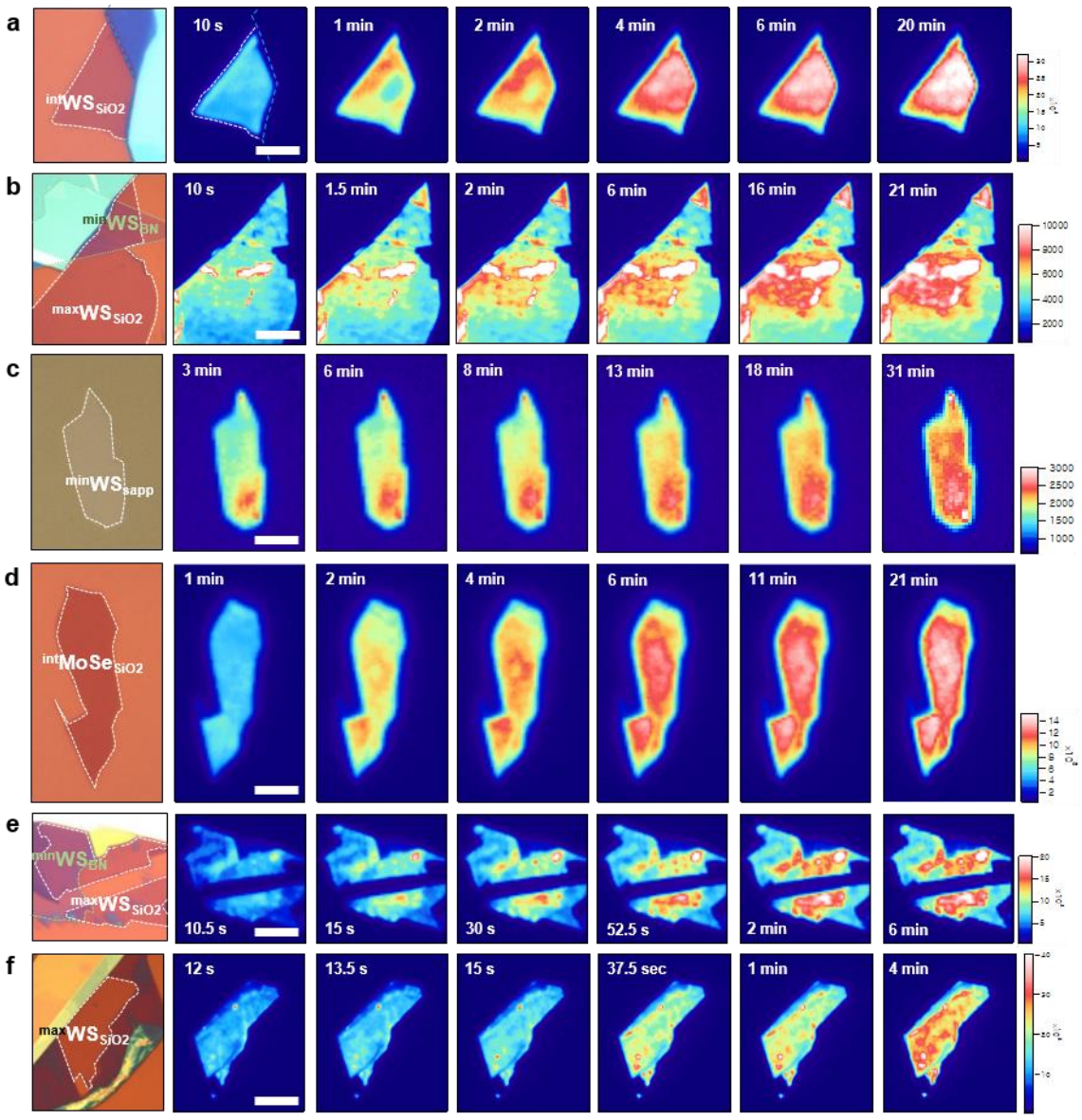

Figure S2. Raw PL images with optical micrographs. (a) $^{int}WS_{SiO2}$ (corresponding to Fig. 3a), (b) $^{max}WS_{SiO2}$ and $^{min}WS_{BN}$ (Fig. 3b), (c) $^{min}WS_{sapp}$ (Fig. 3c), (d) $^{int}MoSe_{SiO2}$ (Fig. S4c), (e) UVO-treated $^{max}WS_{SiO2}$ and $^{min}WS_{BN}$ (Fig. 4a), and (f) UVO-treated $^{max}WS_{SiO2}$ (Fig. 4b). O_2-exposure time is given in each panel. Scale bars are 6, 10, 4, 5, 10, and 7 μm, respectively.

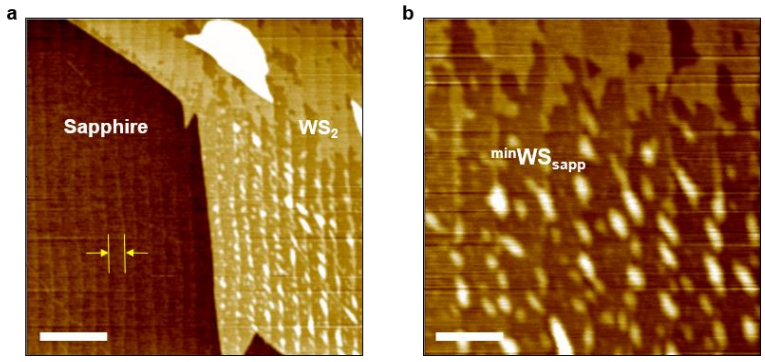

Figure S3. AFM topographic images of $^{min}WS_{sapp}$. The vertical stripes with a spacing of ~300 nm (marked with arrows) in (a & b) are due to the steps between (0001) terraces and water layers localized to the step edges. Scale bars are 1.5 and 0.5 μm, respectively.

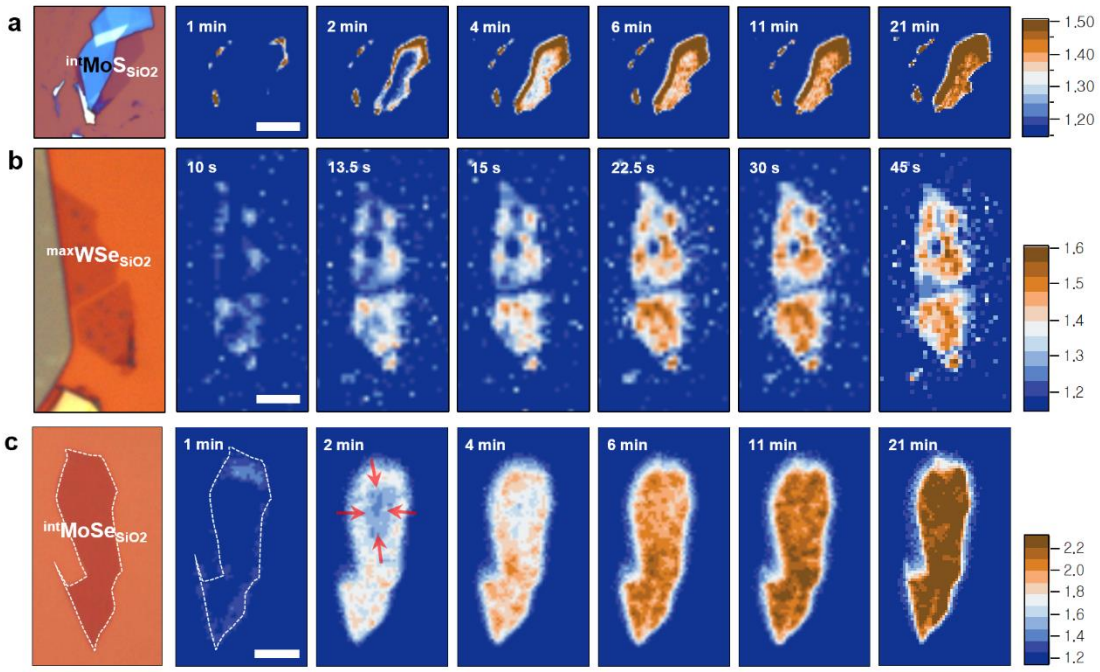

Figure S4. Diffusion-driven CT in MoS_2, WSe_2, and $MoSe_2$. (a ~ b) Optical micrographs (first column) and time-lapse wide-field PL enhancement images $^{int}MoS_{SiO2}$ (a), $^{max}WSe_{SiO2}$ (b), and $^{int}MoSe_{SiO2}$ (c). O_2-exposure time is given in each panel. Scale bars are 7, 4, and 5 μm, respectively.

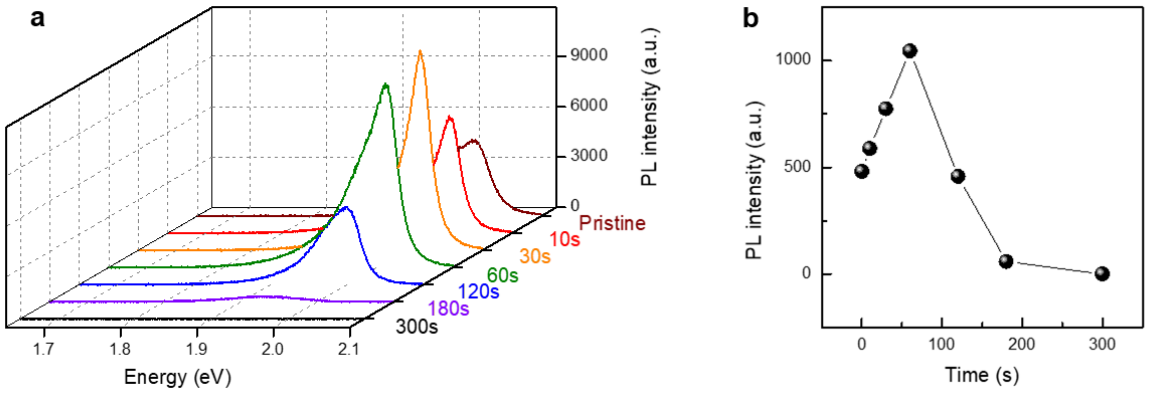

Figure S5. Effects of UVO treatments on PL spectra of $^{int}WS_{SiO2}$. (a & b) PL spectra (a) and their integrated PL intensities (b) before and after UVO treatments for various exposure times.

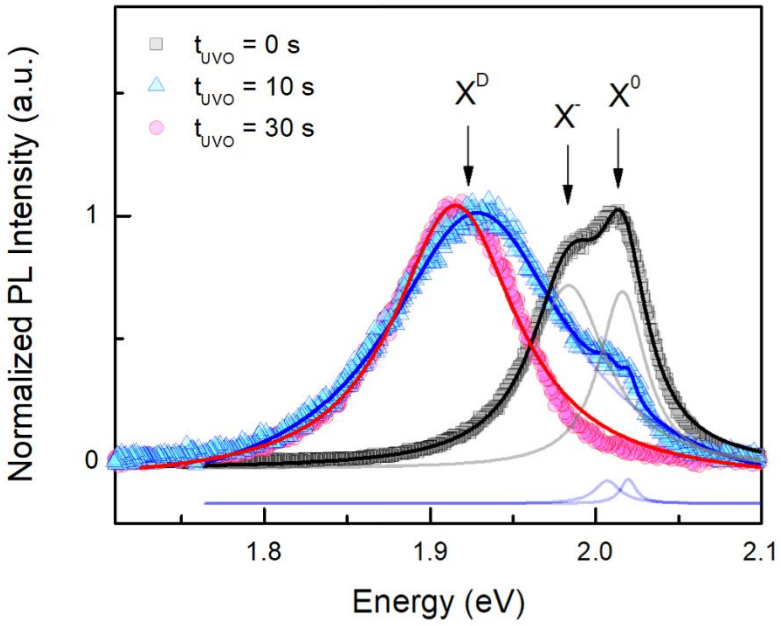

Figure S6. Defect-induced PL peak of UVO-treated $^{int}WS_{SiO2}$. The PL spectra obtained before and after UVO treatments were fitted with a triple-Lorentzian function for the defect-induced peak (X^D), neutral (X^0), and charged excitons (X^-).

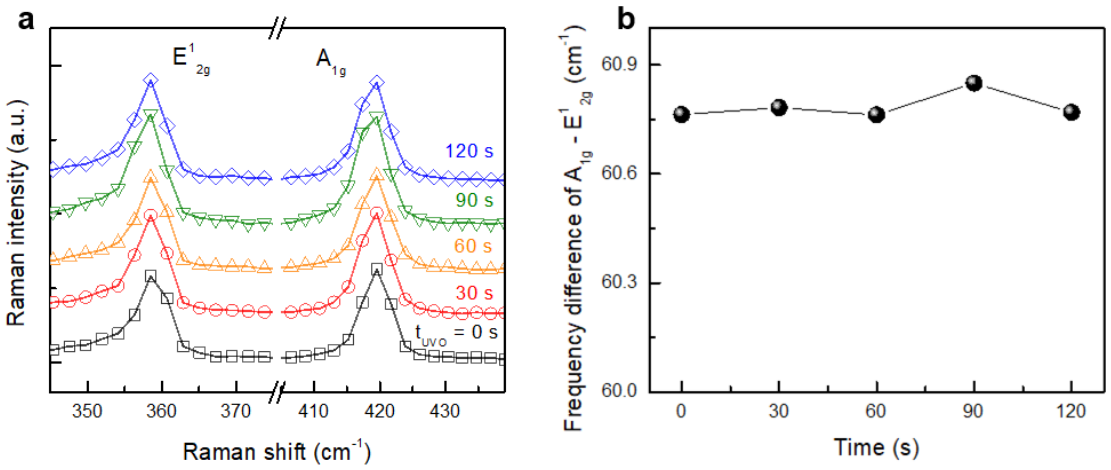

Figure S7. Effects of UVO treatments on Raman spectra of $^{int}WS_{SiO2}$. (a & b) Raman spectra (a) and frequency difference between E^1_{2g} and A_{1g} (b) before and after UVO treatments for various exposure times. Solid lines are double-Lorentzian fits.

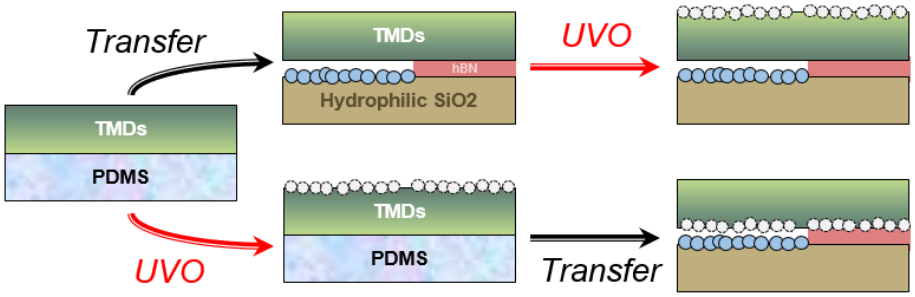

Figure S8. Schematic procedure to prepare $^{max}MX_{SiO2}$ samples with either TMD surface UVO-treated.

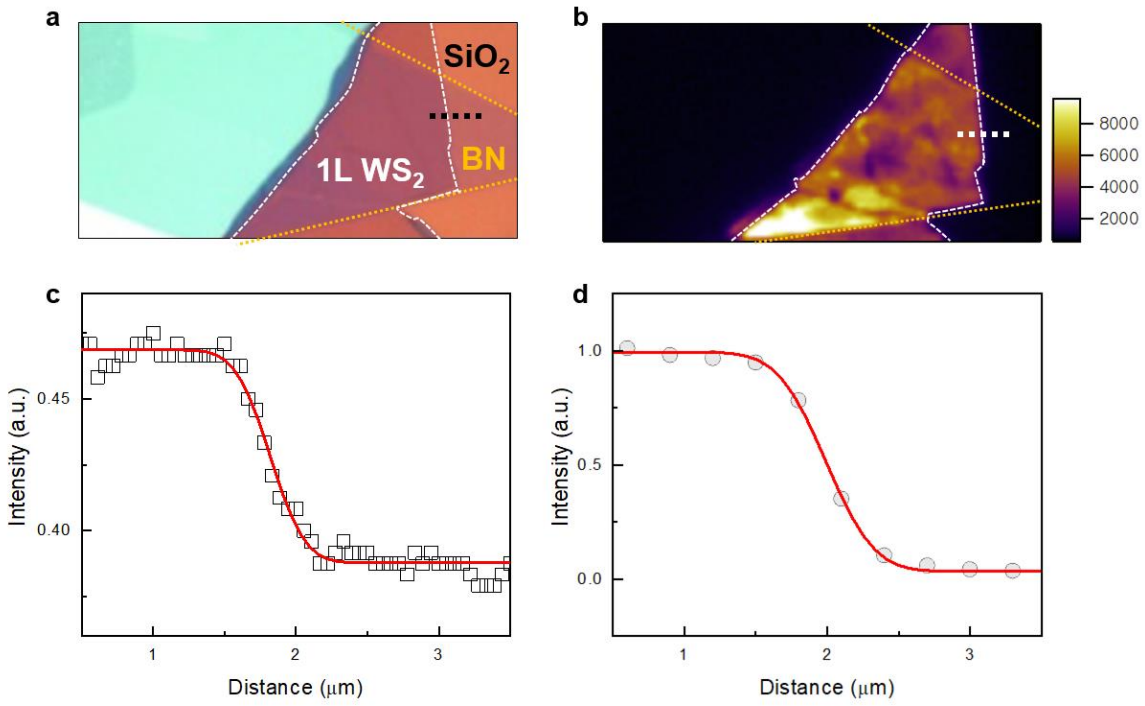

Figure S9. Spatial resolution of wide-field images. (a ~ b) Optical micrograph using a 100X objective (a) and wide-field PL image using a 40X objective (b). (c & d) Intensity profiles extracted from the dashed lines in (a) for red-channel and (b), respectively. The FWHM of Gaussian edge response function (fits in solid red line) was 380 and 530 nm, respectively.

Supplementary Table

Table S1. Change in the electron density of various WS_2 samples induced by CT

	gas conditions	I_{X^-}/I_{X0}	E_{diss} (meV)	n_e (cm^{-2})	Δn_e (cm^{-2})
$^{max}WS_{SiO2}$	Ar	1.2	39	1.3×10^{12}	1.3×10^{12}
	$Ar:O_2$	0.046	33	6.6×10^{10}	
$^{int}WS_{SiO2}$	Ar	3.8	36	4.9×10^{12}	2.8×10^{12}
	$Ar:O_2$	1.3	32	2.0×10^{12}	
$^{min}WS_{BN}$	Ar	2.4	39	2.7×10^{12}	1.9×10^{9}
	$Ar:O_2$	2.0	34	2.7×10^{12}	
$^{min}WS_{sapp}$	Ar	3.6	50	2.7×10^{12}	1.4×10^{12}
	$Ar:O_2$	1.4	44	1.3×10^{12}	